Available online at www.sciencedirect.com

ScienceDirect

www.elsevier.com/locate/jmbbm

Effects of internal pressure and surface tension on the growth-induced wrinkling of mucosae

Wei-Hua Xie[a], Bo Li[b], Yan-Ping Cao[a], Xi-Qiao Feng[a,*]

[a]Institute of Biomechanics and Medical Engineering, AML, Department of Engineering Mechanics, Tsinghua University, Beijing 100084, China

[b]Department of Mechanical Engineering and Johns Hopkins Physical Sciences—Oncology Center, The Johns Hopkins University, Baltimore, Maryland 21218, USA

ARTICLE INFO

Article history:
Received 19 February 2013
Received in revised form
13 May 2013
Accepted 17 May 2013
Available online 25 May 2013

Keywords:
Mucosa
Tissue growth
Surface wrinkling
Surface tension
Internal pressure

ABSTRACT

Surface wrinkling of mucosae is crucial for the biological functions of many living tissues. In this paper, we investigate the instability of a cylindrical tube consisting of a mucosal layer and a submucosal layer. Our attention is focused on the effects of internal pressure and surface tension on the critical condition and mode number of surface wrinkling induced by tissue growth. It is found that the internal pressure plays a stabilizing role but basically has no effect on the critical mode number. Surface tension also stabilizes the system and reduces the critical mode number of surface patterns. Besides, the thinner the mucosal layer, the more significant the effect of surface tension. This work may help gain insights into the surface wrinkling and morphological evolution of such tubular organs as airways and esophagi.

1. Introduction

The growth and morphogenesis of biological tissues and organs are mediated not only by genetic factors but also by environmental effects, e.g. chemical concentrations and mechanical forces (Taber, 1995; Jones and Chapman, 2012; Li et al., 2012). For example, the early development of solid tumors is distinctly affected by the diffusion of nutrient chemicals within the extracellular matrix. The inhomogeneous distribution of nutrients, caused by such reasons as the consumption of tumors themselves, may engender nonuniform cell proliferation and, consequently, elicit specific structures (e.g., a central necrotic core observed in human cervical carcinoma spheroid) and mechanical stresses (Sutherland, 1988; Tracqui, 2009). It has been believed that these intrinsic stresses incurred by differential volumetric growth closely associate with irregular surface patterns on the tumors and their invasion into host tissues (Dervaux et al., 2011; Pham et al., 2011; MacLaurin et al., 2012). As a matter of fact, growth-induced stresses regulate the morphogenesis of almost all biological things in the realms ranging from plants to animals (Liang and Mahadevan, 2009; Li et al., 2011a, 2011c; Savin et al., 2011; Li et al., 2012).

In the past decades, much effort has been directed towards understanding the formation of surface patterns in a diversity of biological tissues and the underlying physical mechanisms. As a class of typical soft tissues, mucous membranes (or mucosae) exist in the inner surfaces of many living organisms, e.g., airways, arteries, esophagi, stomachs and gastrointestinal tracts. Mucosae grow in the way of volumetric variations and are featured by different surface wrinkles and ridges (Lambert et al., 1994; Taber, 1995; Wiggs

*Corresponding author. Tel.: +86 10 62772934; fax: +86 10 62781824.
E-mail address: fengxq@tsinghua.edu.cn (X.-Q. Feng).

1751-6161/$ - see front matter © 2013 Elsevier Ltd. All rights reserved.
http://dx.doi.org/10.1016/j.jmbbm.2013.05.009

et al., 1997; Fayed et al., 2010). Such patterns are reminiscent of those induced by buckling in such mechanical systems as a stiff film anchored on a compliant substrate. This kind of composite systems may buckle and evolve into various morphologies when the compressive stress in the film exceeds a critical value (Tanaka et al., 1987; Sultan and Boudaoud, 2008; Breid and Crosby, 2009; Liu et al., 2010). Surface patterns not only play a significant role in many physiological functions of healthy tissues but also are clinically relevant to some diseases (e.g. asthma, inflammation, edema and lymphoma) and, hence, their variations have also been regarded as a pathological phenotype (Wiggs et al., 1997).

Due to its physiological and pathological relevance, surface wrinkling of mucosae has received much attention (Lambert et al., 1994; Hrousis et al., 2002; Yang et al., 2007). Recently, Li et al. (2011b) performed a linear perturbation analysis on the growth-induced wrinkling of esophagi and airways. Moulton and Goriely (2011) studied the circumferential buckling instability of a growing cylindrical tube under an external pressure. These previous studies showed that the wrinkling patterns of mucosae are dictated by geometrical and physical parameters of the system, e.g. the thicknesses and mechanical properties of the mucosal and submucosal layers (Wiggs et al., 1997; Li et al., 2011b). In such tubular organs as airways and esophagi, which have an essential function of transportation, there always exists air or liquid. The intraluminal fluids exert an internal pressure on the inner surface of the organs. In addition, the inner mucosal layer has a pronounced surface tension (Hill et al., 1997; Heil and White, 2002; Heil et al., 2008). Experimental observation in airways suggests that surface tension is closely relevant to the closure and opening of airways (Burger and Macklem, 1968; Heil et al., 2008). Kang and Huang (2010) showed that surface tension may modulate the critical wavelength and the critical swelling ratio at the onset of surface instability induced by water-sucking in a planar hydrogel layer. To date, however, the effects of internal pressure and surface tension on the surface wrinkling of growing cylindrical tubes remain unclear.

In this paper, we will investigate, through combined theoretical analysis and numerical simulations, the effects of internal pressure and surface tension on the stability of airways and esophagi. The critical wrinkling condition and the characteristic mode number of the induced surface pattern in the growing system are explored. This paper is organized as follows. In Section 2, a theoretical model is presented to analyze the growth behavior of mucosae and submucosae with the effects of internal pressure and surface tension. A linear perturbation analysis is performed in Section 3 to predict the critical conditions of wrinkling. Nonlinear finite element simulations are also conducted to verify our analytical solution. The implications and conclusions drawn from the present study are given in Section 4.

2. Model of volumetric growth

2.1. Deformation and stress analysis

Such tubular organs as pulmonary airways and esophagi have a multiple-layered structure, which can be roughly divided into three layers, including an innermost mucosal membrane and a submucosal layer enveloped by a stiff muscular layer (Li et al., 2011b). In this paper, therefore, we consider an isotropic and hyperelastic cylinder containing a mucosal layer and a submucosal layer, which grow either in a fixed tube or without any external constraint. Usually, mucosae are much stiffer than submucosae. Therefore, we assume that the elastic modulus of the mucosa is higher than that of the submucosa. The volumetric growth model originally established by Rodriguez et al. (1994) is employed to analyze growth-induced deformation. In the cylindrical coordinate system, the position of a representative material point at the initial configuration $\mathbf{X}=(\mathrm{R},\Theta,\mathrm{Z})$ transforms to $\mathbf{x}=(r,\theta,z)$ at the current configuration due to tissue growth, as shown in Fig. 1. The bilayer tube has the initial inner radius A, the interface radius B, and the outer radius C. Thus, the initial thicknesses of the mucosal layer and the submucosal layer are $H_m=B-A$ and $H_s=C-B$, respectively. Here and in the sequel, the subscripts m and s denote the quantities defined in the mucosa and submucosa, respectively.

Consider the case of axisymmetric growth, which would lead to axisymmetric deformation, i.e. $r=r(\mathrm{R})$. In the current configuration, the inner, interfacial and outer radii become a, b and c, respectively. The associated deformation gradient tensor is written as $\mathbf{F}=\partial\mathbf{x}/\partial\mathbf{X}=diag(\lambda_1,\lambda_2,\lambda_3)$, where $\lambda_1=\partial r/\partial\mathrm{R}$, $\lambda_2=r/\mathrm{R}$ and λ_3 are the three principal stretches. Here and in the sequel, the indices 1, 2 and 3 stand for the radial, circumferential, and axial directions, respectively. According to the volumetric growth theory (Rodriguez et al., 1994; Ben Amar and Goriely, 2005), the deformation gradient $\mathbf{F}$ can be decomposed into $\mathbf{F}=\mathbf{A}\cdot\mathbf{G}$, where $\mathbf{G}$ denotes the growth part and $\mathbf{A}$ the elastic deformation part. The growth tensor is assumed as $\mathbf{G}=diag(g_1,g_2,g_3)$, where $g_i(i=1,2,3)$ denote the growth factor in the i-th direction, with $g_i>1$ representing growth and $0<g_i<1$ shrinkage. Assume that the bilayer deforms and grows under the plane-strain conditions, that is, the deformation and growth do not happen in the longitudinal direction. Thus the growth tensor reduces to $\mathbf{G}=diag(g_1,g_2,1)$ and the deformation gradient tensor has the form of $\mathbf{F}=diag(\lambda_1,\lambda_2,1)$. We further assume g_1 and g_2 to be spatially uniform and only consider the isotropic growth, i.e. $g_1=g_2=g>1$. The elastic deformation tensor $\mathbf{A}$ has the form of $\mathbf{A}=diag(\alpha_1,\alpha_2,\alpha_3)$, where the stretch ratios are $\alpha_1=g^{-1}\partial r/\partial\mathrm{R}$, $\alpha_2=g^{-1}r/\mathrm{R}$ and $\alpha_3=1$. In general, the elastic deformation of living soft tissues yields little volume change. Therefore, the nonlinear responses of mucosae and submucosae can be described by the isotropic and incompressible

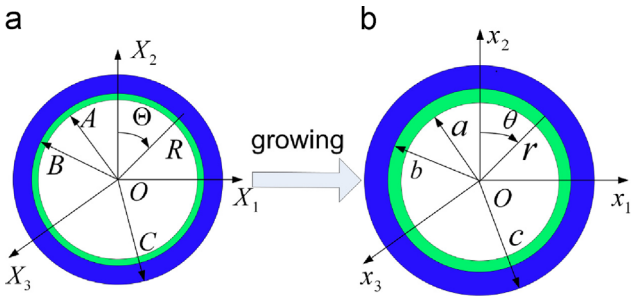

Fig. 1 – A growing bilayer tissue in a cylindrical lumen: (a) initial configuration and (b) current configuration.

neo-Hookean constitutive relation with the strain energy function $W=\mu(\alpha_1^2+\alpha_2^2+\alpha_3^2-3)/2$, where μ is the shear modulus at the ground state. The incompressibility implies the determinant of the elastic deformation tensor $det(\mathbf{A})=1$, which yields $\alpha_2=\alpha_1^{-1}=\alpha$. The incompressibility condition also requires $det(\mathbf{F})=det(\mathbf{G})$, which leads to $rR^{-1}\partial r/\partial R=g^2$. Using this relation and the interface continuity conditions, the deformations in the mucosal and submucosal layers are derived as

$$r^2-a^2=g_m^2(R^2-A^2)\quad (A\le R\le B), \tag{1}$$

$$r^2-c^2=g_s^2(R^2-C^2)\quad (B\le R\le C). \tag{2}$$

The interface between the mucosal and submucosal layers is assumed to be perfectly bonded. Thus the displacements and the normal stress are continuous across the interface. The continuity condition of displacement requires that

$$r(B)|_m=r(B)|_s. \tag{3}$$

Once the inner radius a or the outer radius c is known, the deformation fields in the mucosal and submucosal layers can be determined.

In the cylindrical coordinate system, the equilibrium equation reads

$$\frac{\partial\sigma_{rr}}{\partial r}+\frac{1}{r}(\sigma_{rr}-\sigma_{\theta\theta})=0, \tag{4}$$

where σ_{rr} and $\sigma_{\theta\theta}$ are the radial and circumferential components of the Cauchy stress tensor (Ogden, 1984). For incompressible hyperelastic materials, the constitutive law obeys

$$\boldsymbol{\sigma}=\mathbf{A}\cdot\frac{\partial W}{\partial\mathbf{A}}-p\mathbf{I}, \tag{5}$$

where p is a Lagrangian multiplier ensuring elastic incompressibility. Hence, we have

$$\sigma_{rr}=\mu\alpha^{-2}-p,\ \sigma_{\theta\theta}=\mu\alpha^2-p. \tag{6}$$

Solving Eqs. (4) and (6) under specified boundary conditions, the deformations and stresses caused by the volumetric growth can be obtained. In the presence of internal pressure and surface tension, the solutions will be shown in Subsections 2.2 and 2.3, respectively.

2.2. Solution with the effect of internal pressure

We first derive the solution of displacements and stresses in the presence of an internal pressure T acting on the inner surface of mucosa. Two representative boundary conditions at $r=c$ are considered, namely (i) the fixed boundary condition and (ii) the traction-free boundary condition.

By replacing the variable r by α, the equilibrium equation in (4) reduces to

$$\frac{\partial\sigma_{rr}}{\partial\alpha}=-\mu(\alpha^{-1}+\alpha^{-3}) \tag{7}$$

The traction boundary condition at the inner surface ($r=a$) is

$$\sigma_{rr}(\alpha_{am})=-T, \tag{8}$$

where α_{am} represents the stretch ratio at $r=a$.

From Eqs. (1) and (2), the outer boundary condition at $r=c$, and the continuity condition at the interface, one obtains

$$a=\left[C^2-g_m^2(B^2-A^2)-g_s^2(C^2-B^2)\right]^{1/2}. \tag{9}$$

When the outer boundary at $r=c$ is fixed, the stresses in the bilayer cylindrical tube are derived from Eqs. (7) and (8) as

$$\begin{aligned}&\sigma_{rrm}=-T+\tfrac{\mu_m}{2}\left[(\alpha_m^{-2}-\alpha_{am}^{-2})+\ln\tfrac{\alpha_{am}^2}{\alpha_m^2}\right],\\&\sigma_{\theta\theta m}=\sigma_{rrm}+\mu_m(\alpha_m^2-\alpha_m^{-2})\qquad (A\le R\le B),\end{aligned} \tag{10}$$

$$\begin{aligned}&\sigma_{rrs}=\sigma_{rrm}\Big|_{\alpha_m=\alpha_{bm}}+\tfrac{\mu_s}{2}\left[(\alpha_s^{-2}-\alpha_{bs}^{-2})+\ln\tfrac{\alpha_{bs}^2}{\alpha_s^2}\right],\\&\sigma_{\theta\theta s}=\sigma_{rrs}+\mu_s(\alpha_s^2-\alpha_s^{-2})\qquad (B\le R\le C),\end{aligned} \tag{11}$$

where

$$\begin{aligned}&\alpha_{am}\equiv\tfrac{a}{g_m A}=\left[\tfrac{C^2}{g_m^2A^2}-\tfrac{g_s^2}{g_m^2A^2}(C^2-B^2)-\left(\tfrac{B^2}{A^2}-1\right)\right]^{1/2},\\&\alpha_{bm}\equiv\tfrac{b}{g_m B}=\left[\tfrac{C^2}{g_m^2B^2}-\tfrac{g_s^2}{g_m^2}\left(\tfrac{C^2}{B^2}-1\right)\right]^{1/2},\\&\alpha_{bs}\equiv\tfrac{b}{g_s B}=\left[\tfrac{C^2}{g_s^2B^2}-\left(\tfrac{C^2}{B^2}-1\right)\right]^{1/2}.\end{aligned} \tag{12}$$

When $T=0$, the above solution degenerates to that without internal pressure (Li et al., 2011b). It is found that when the outer boundary is fixed, the only difference between the two solutions lies in the term $-T$ in all normal stresses in Eqs. (11) and (12), indicating that the internal pressure simply causes a uniform hydrostatic stress field $\sigma_{ij}=-T\delta_{ij}$ in the whole system. The reason lies in that both the mucosa and submucosa are assumed to be incompressible in our analysis. In this case, when the outer boundary is fixed, the internal pressure cannot cause any extra deformation in the system.

In the case when the outer boundary is traction free at $r=c$, the following relation for the internal pressure can be derived from Eq. (7):

$$T=-\int_{\alpha_a}^{\alpha_c}\mu(\alpha^{-1}+\alpha^{-3})d\alpha. \tag{13}$$

For a given pressure T, Eqs. (1)–(3) and (13) constitute a closed equation system to solve a and α_{am}.

2.3. Solution with the effect of surface tension

Now we consider the effect of surface tension in the inner surface ($r=a$) under two outer boundary conditions: (i) fixed (i.e. $r(C)=C$) and (ii) traction-free. The stress boundary condition at $r=a$ reads (Dervaux and Ben Amar, 2011).

$$\boldsymbol{\sigma}\cdot\mathbf{n}=\kappa\gamma\mathbf{n}, \tag{14}$$

where κ is the curvature at $r=a$ in the current configuration, γ is the surface tension, and $\mathbf{n}$ the unit outward vector normal to the current boundary. Before the occurrence of wrinkling, one has $\kappa=1/a$.

When the outer boundary is fixed, by using the condition $r(C)=C$, it is known that the displacement field also satisfies Eq. (9). Using the equilibrium equation in Eq. (7) and the boundary conditions, the growth-induced stress fields in the mucosal and submucosal layers are obtained as

$$\begin{aligned}&\sigma_{rrm}=-\tfrac{\gamma}{a}+\tfrac{\mu_m}{2}\left[(\alpha_m^{-2}-\alpha_{am}^{-2})+\ln\tfrac{\alpha_{am}^2}{\alpha_m^2}\right],\\&\sigma_{\theta\theta m}=\sigma_{rrm}+\mu_m(\alpha_m^2-\alpha_m^{-2})\qquad (A\le R\le B),\end{aligned} \tag{15}$$

$$\sigma_{rrs}=\sigma_{rrm}\Big|_{\alpha_m=\alpha_{bm}}+\tfrac{\mu_s}{2}\left[(\alpha_s^{-2}-\alpha_{bs}^{-2})+\ln\tfrac{\alpha_{bs}^2}{\alpha_s^2}\right],$$

$$\sigma_{\theta\theta s} = \sigma_{rrs} + \mu_s\left(\alpha_s^2 - \alpha_s^{-2}\right) \qquad (B \le R \le C), \tag{16}$$

where the expressions of α_{am}, α_{bm} and α_{bs} are the same as Eq. (12).

When the outer boundary is traction free at $r = c$, Eq. (13) still holds for the internal pressure in the system.

3. Wrinkling analysis

3.1. Linear perturbation method

The buckling behavior of the cylindrical tube is here analyzed by invoking an incremental deformation theory (Ogden, 1984; Ben Amar and Goriely, 2005; Li et al., 2011a; Li et al., 2011b). Previously, we have performed a linear perturbation analysis to predict the stability of deformation (Li et al., 2011b). Following the same procedure, we here study the effects of internal pressure and surface tension on the critical condition of wrinkling and the induced surface patterns. In the analysis, the current configuration is chosen as the reference configuration, in which the displacement perturbation will be specified.

The incremental equilibrium equation is

$$\operatorname{div} \dot{\mathbf{S}}_0 = 0, \tag{17}$$

where $\dot{\mathbf{S}}_0$ is the incremental nominal stress tensor.

Surface wrinkling occurs when the deformation in the system bifurcates into a non-axisymmetric mode. In the linear stability analysis, we assume that the incremental displacements along the radial and circumferential directions have the form of

$$u = \tilde{u}(r)\cos n\theta, \quad v = \tilde{v}(r)\sin n\theta, \tag{18}$$

where n is the circumferential mode number of wrinkling and $\tilde{u}$ and $\tilde{v}$ are the functions of r. Using the condition of incompressibility, the incremental equilibrium condition (17) reduces to a fourth-order differential equation (Li et al., 2011b), which, in conjunction with the four boundary conditions at $r = a$ and $r = c$ and the continuity conditions at interface $r = b$, constitute a closed system of equations. Wrinkling will happen when the differential system has a non-trivial solution. We employ the fourth-order Runge–Kutta method to numerically solve the differential system and the determinantal method to obtain the critical condition and mode number of surface wrinkling (Ben Amar and Goriely, 2005; Li et al., 2011a, 2011b).

3.2. Effect of internal pressure

Now we examine the effect of internal pressure on the wrinkling behavior. At the fixed outer surface ($r = c$), the incremental displacement boundary condition reads

$$\dot{\mathbf{x}} = \mathbf{0} \tag{19}$$

At the inner free surface ($r = a$), the traction boundary condition is (Ogden, 1984)

$$\dot{\mathbf{S}}_0^{\mathrm{T}} \cdot \mathbf{n} = -\dot{T}\mathbf{n}, \tag{20}$$

where $\dot{T}$ denotes the increment of the internal pressure. Assume that the internal pressure keeps constant during deformation, that is, $\dot{T} = 0$. Since the deformations in the mucosal and submucosal layers are independent of T, as demonstrated in Subsection 2.2, the internal pressure has no influence on the stability of the tubular structure when the outer surface is fixed.

In what follows, we will mainly investigate the case where the outer boundary is traction-free. For illustration, assume that the mucosa undergoes an isotropic growth and the submucosa does not grow, that is, $g_{1m} = g_{2m} = g$ and $g_{1s} = g_{2s} = 1$. When the mucosa and submucosa grow simultaneously, the problem can be analyzed similarly. The internal pressure is normalized as $\Pi = T/\mu_s$. The following representative parameters are used: $H_m/C = 0.005$, $H_s/C = 0.5$, and $\mu_m/\mu_s = 50$.

Corresponding to an arbitrary value of the mode number n, the mucosal growth factor g at the onset of wrinkling can be determined from the linear perturbation method described above. Under several given values of Π, Fig. 2 shows the curves of g as a function of n. Among all possible wrinkling patterns, there exists a minimum value of g in each curve, which would minimize the elastic strain energy of the system. This value, denoted as g_{crit}, is deemed as the critical growth factor of wrinkling, and the corresponding mode number, n_{crit}, is the critical mode number of surface pattern. It can be seen from Fig. 2 that as the internal pressure increases, the critical growth factor g_{crit} increases but the critical mode number n_{crit} remains constant. This suggests that the internal pressure tends to stabilize the system but basically has no effect on the wrinkling pattern.

Figs. 3a and b respectively depict the variations of the critical growth factor g_{crit} and the critical mode n_{crit} with respect to the modulus ratio μ_m/μ_s, where we take $H_m/C = 0.005$ and $H_s/C = 0.5$. When the modulus ratio is in a moderate range (e.g., $\mu_m/\mu_s < 50$), the critical growth factor decreases rapidly with increasing μ_m/μ_s. When the mucosa is much stiffer than the submucosa (e.g., $\mu_m/\mu_s > 100$), the critical growth factor increases slightly with the increase in μ_m/μ_s. This result can be qualitatively understood as follows. When the mucosa is moderately stiffer than the submucosa, instability manifests itself in a localized way and, in other words, wrinkling occurs only at the inner surface of the mucosal layer. In this case, the bilayer system with a larger value of μ_m/μ_s will be easier to wrinkle. This is consistent with the conclusion in the absence of internal pressure (Li et al., 2011b). However, when the ratio μ_m/μ_s is sufficiently large, the

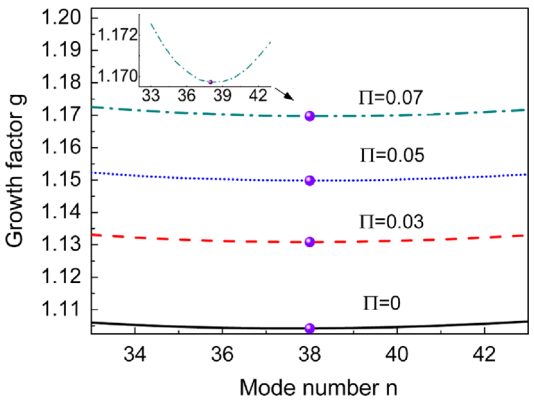

Fig. 2 – Relation between the mode number of surface pattern and the corresponding growth factor of wrinkling.

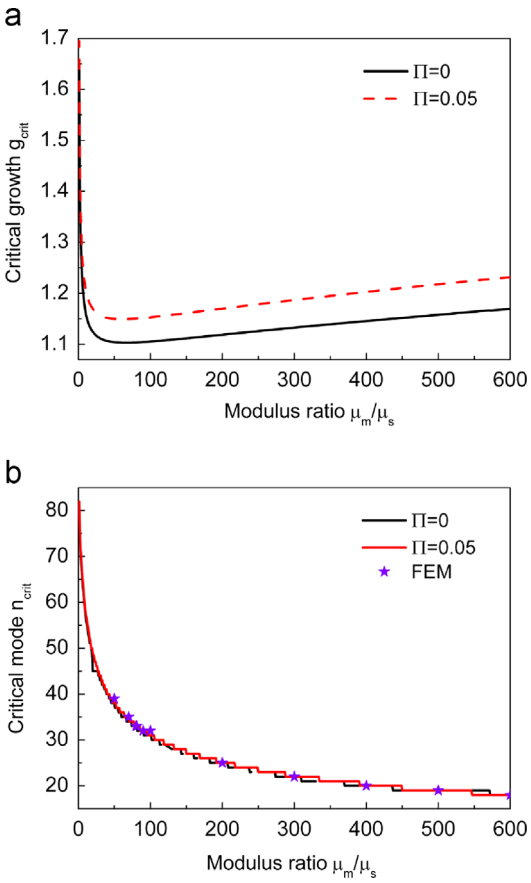

Fig. 3 – Effect of the modulus ratio μ_m/μ_s on (a) the critical growth factor g_{crit} and (b) the critical mode n_{crit}. The solutions with an internal pressure ($\Pi = 0.05$) are compared with those without internal pressure ($\Pi = 0$). The stars represent the results of finite element simulations.

elastic strain energy of mucosa will dominate the stability of the system since the outer surface of the structure is traction-free. In this case, instability would take place in a global way similar to the buckling of a bilayer ring. Thus, the composite structure with a larger mucosal stiffness will become more difficult to wrinkle.

To validate the above theoretical results, we perform finite element simulations using the commercial finite element software, ABAQUS (Version 6.10-1). About 24,000 eight-noded plane-strain hybrid elements (CPE8RH) are used in the whole system. The mesh is sufficiently fine to ensure the mesh-independence of the calculation results. Under the traction-free boundary condition on the outer surface, the growth-induced buckling in the bilayer tube with an internal pressure T is simulated. Assume that as the mucosal layer grows, the submucosa does not grow and plays a restricting role, rendering a compressive stress in the growing mucosal layer. When the circumferential compressive stress reaches a critical condition, the mucosa becomes unstable and buckles into a sinusoidal pattern, as shown in Figs. 4b and c. It can be seen from Fig. 3b that the numerical results have a good agreement with our theoretical solution. The finite element method also reveals that an increasing modulus ratio μ_m/μ_s tends to decrease the critical mode number n_{crit}. The comparison between the results with and without internal pressure shows that the internal pressure basically has no effect on the critical mode number of surface pattern.

Furthermore, the effect of internal pressure on the morphological evolution during postbuckling is also explored via finite element simulations. A sequence of deformations in the system with the increase in the growth factor are shown in Figs. 4(a–e), where the geometric and physical parameters are taken as $A = 90$, $B = 90.5$, $C = 200$, $\mu_m/\mu_s = 1000$ and $\Pi = 0.033$. In real biological organs, the ratio between the

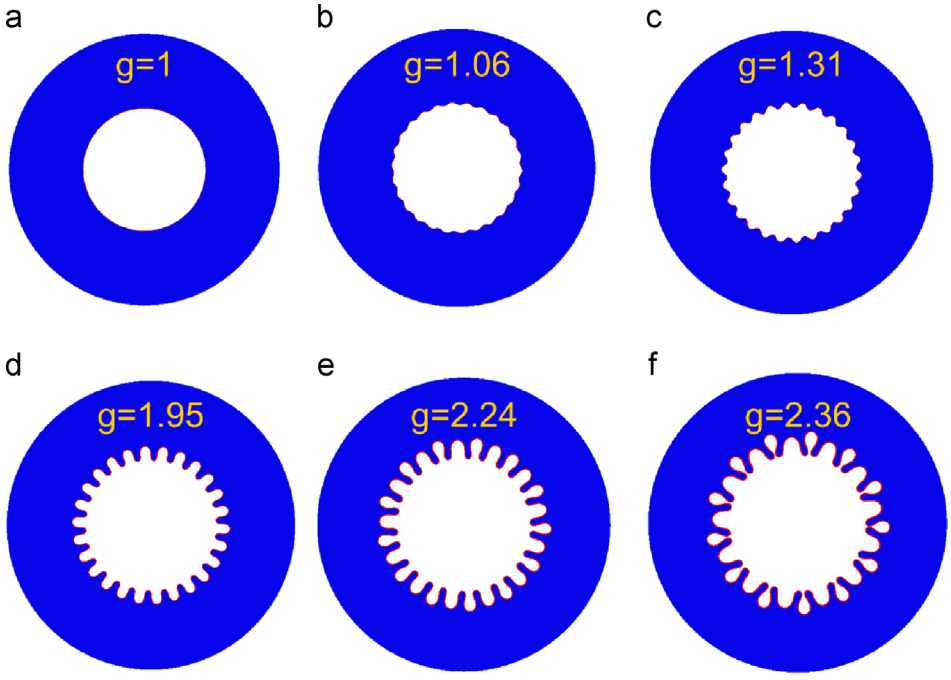

Fig. 4 – Morphological evolution of a cylindrical mucosa–submucosa system with the growth of the mucosal layer, where the internal pressure is set as $\Pi = 0.033$.

elastic moduli of mucosa and submucosa may vary in a broad range. For example, it was taken in the range of 1–314 by Hrousis et al. (2002). When other representative geometric and material parameters are used in the calculation, the morphological evolution induced by the volumetric growth is similar to that in Fig. 4.

The deformation process shown in Fig. 4 can be divided into three stages. In the first stage, the cylindrical tube grows in an axisymmetric manner and keeps the cylindrical symmetry. With the growth of the mucosa, the circumferential compressive stress becomes higher and higher. In the second stage, the first bifurcation occurs and the system buckles into a non-axisymmetric morphology when the compressive stress reaches a critical condition. A sinusoidal wrinkling pattern forms on the inner surface (Figs. 4b and c), as predicted by the above theoretical analysis. With further growth of the mucosa, the wavy wrinkles become deeper and deeper, leading to a finger-like pattern (Fig. 4d). If the mucosa is much stiffer than the submucosa, the system may undergo a secondary bifurcation during postbuckling, entering into the third stage. One wrinkle grows in amplitude at the expense of the amplitudes of its two neighbors. The second bifurcation creates a period-doubling morphology (Fig. 4e) and, in turn, a pitchfork-like pattern (Fig. 4f). This wrinkle-to-fold transition releases a part of the elastic strain energy of the system.

By comparing the postbuckling processes with and without internal pressure, it can be found that the morphology evolutions for the two cases are quite similar (Li et al., 2001b). However, both the first and second bifurcations are delayed due to the presence of an internal pressure, demonstrating its stabilizing role in the buckling process.

3.3. *Effect of surface tension*

In this subsection, we examine the effects of surface tension on the critical condition and the circumferential mode number of surface wrinkling. At the onset of sinusoidal wrinkling, the curvature of the inner mucosal surface ($r=a$) has the following perturbation:

$$\dot{\kappa}=\frac{1}{a^2}\left(n^2-1\right)\tilde{u}(r)\cos\, n\theta. \tag{21}$$

Correspondingly, the incremental boundary condition reads

$$\dot{\mathbf{S}}_0^{\,T}\cdot\mathbf{n}=\dot{\kappa}\gamma\mathbf{n}-\kappa\gamma\dot{\mathbf{F}}_0^{\,T}\cdot\mathbf{n}, \tag{22}$$

where $\dot{\mathbf{F}}_0$ is the incremental deformation tensor.

For illustration, we set $H_m/C=0.005$, $H_s/C=0.5$, and $\mu_m/\mu_s=50$. The growth mode is taken as $g_{1m}=g_{2m}=g$ and $g_{1s}=g_{2s}=1$. The normalized parameter $\Gamma=\gamma/(A\mu_m)$ is employed to characterize the effect of surface tension.

Under the traction-free outer boundary condition, the relations between the surface pattern mode number n and the corresponding growth factor g are plotted in Fig. 5 for several values of surface tension Γ. It is seen that with the increase in Γ, the critical growth factor g_{crit} increases while the critical mode number n_{crit} decreases. A positive surface tension, which manifests itself through the curvature at the mucosal surface, tends to suppress the crests and to shallow

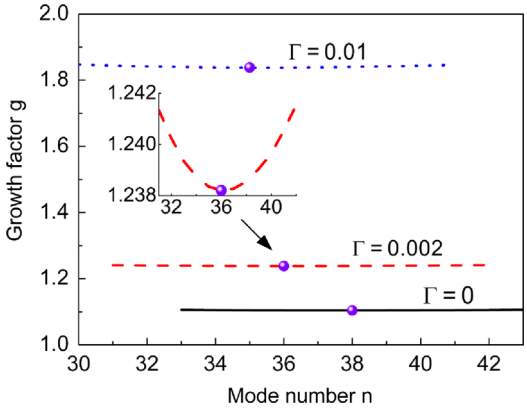

Fig. 5 – Effect of surface tension on the wrinkling behavior of a cylindrical mucosa–submucosa system.

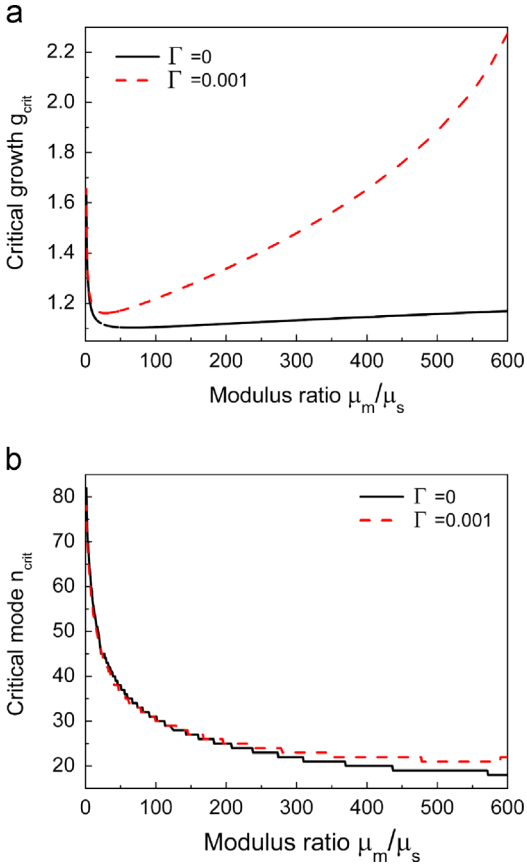

Fig. 6 – Dependence of (a) the critical growth factor g_{crit} and (b) the critical surface pattern mode n_{crit} on the modulus ratio μ_m/μ_s under several representative values of surface tension in the case of traction-free outer boundary condition.

the troughs of wave-like perturbation at the inner surface. Therefore, surface tension increases the wavelength of the surface pattern or, in other words, decreases the mode number.

The effects of the modulus ratio μ_m/μ_s on the critical growth factor g_{crit} and the critical mode number n_{crit} are shown in Fig. 6 under the traction-free outer boundary condition, where we take $H_m/C=0.005$ and $H_s/C=0.5$. In this

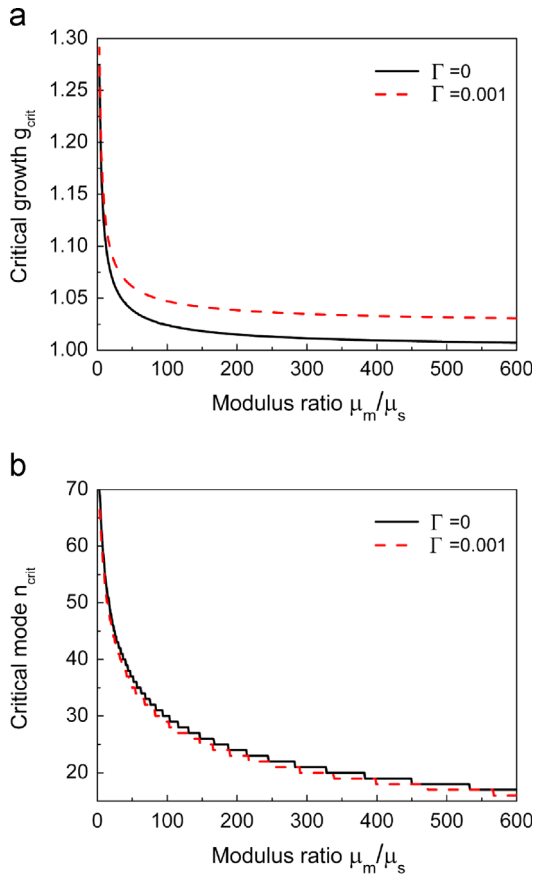

Fig. 7 – Dependence of (a) the critical growth factor g_{crit} and (b) the critical surface pattern mode n_{crit} on the modulus ratio μ_m/μ_s under several representative values of surface tension in the case of fixed outer boundary condition.

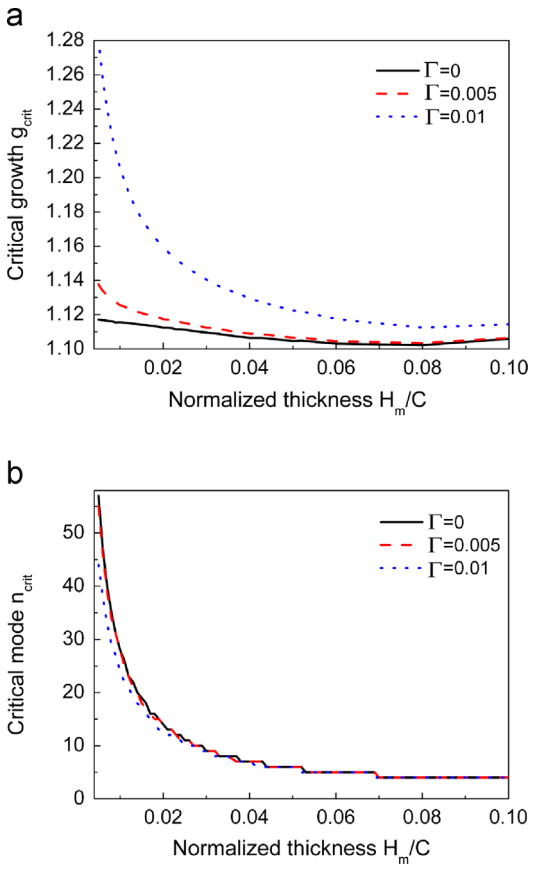

Fig. 8 – Dependence of (a) the critical growth factor g_{crit} and (b) the critical surface pattern mode n_{crit} on the normalized thickness H_m/C under several different values of surface tension.

case, the critical growth factor g_{crit} decreases rapidly with the increase in the modulus ratio μ_m/μ_s when it is relatively small (i.e. $\mu_m/\mu_s<10$). When the mucosa is much stiffer than the submucosa (e.g., $\mu_m/\mu_s>50$), g_{crit} increases with increasing μ_m/μ_s (Fig. 6a). Fig. 6b shows that the critical mode number n_{crit} decreases with the increase in μ_m/μ_s. In addition, it is found that the effect of surface tension on n_{crit} is insignificant.

Under the fixed outer boundary condition, the effects of the modulus ratio μ_m/μ_s on the critical growth factor g_{crit} and the critical mode number n_{crit} are illustrated in Fig. 7, where we take $H_m/C=0.005$ and $H_s/C=0.5$. Clearly, both the critical growth factor g_{crit} and the critical mode number n_{crit} decrease with the increase in μ_m/μ_s. The presence of surface tension tends to increase the value of g_{crit} and slightly lower n_{crit}, indicating a stabilizing role of Γ.

Fig. 8 shows the effect of the mucosal thickness H_m/C on the wrinkling behavior of the bilayer system with the outer boundary condition being fixed, where we take $H_s/C=0.5$ and $\mu_m/\mu_s=10$. As the mucosal layer gets thicker, both the critical growth g_{crit} and the critical mode n_{crit} decrease. By comparing the curves with different surface tensions, we find that when the mucosal layer is very thin, the critical growth g_{crit} increases while the critical mode number n_{crit} decreases with the increase in Γ. Therefore, for a thinner mucosal layer, the effect of surface tension is more significant.

4. Conclusions

Recently, much effort has been directed towards understanding the correlation between the morphology and growth of soft biological tissues (Lambert et al., 1994; Li et al., 2011b). The bilayered cylindrical tube provides a prototype to study the growth of airways, intestines, blood vessels and many other soft tissues or organs. In these systems, the inner surfaces, composed mainly of a mucosal layer, are usually featured by various wrinkles. The present paper is aimed to study the formation of surface wrinkles in such a growing tubular structure via theoretical analysis and finite element simulations. Our main attention has been paid to the effects of internal pressure and surface tension on the critical condition of surface wrinkling and the induced surface pattern mode. It is found that the internal pressure tends to stabilize the system but essentially has no effect on the critical mode number of wrinkling pattern. A positive surface tension also plays a stabilizing role and tends to increase both the critical growth factor and the induced surface pattern wavelength. In addition, the thinner the mucosa, the more significant the effect of surface tension. These results provide insights into the wrinkling behavior of mucosae in a more real physiological environment.

Though only plane-strain problems have been addressed in the present paper, this model can further examine the case with both axial and circumferential growth, which may cause the formation of three-dimensional wrinkles (Li et al., 2009). In addition, the methodology developed in this paper can be applied to other systems, such as soft elastomers or polymeric gels. For instance, the growth-induced deformation and buckling behavior of blood vessels can be studied by introducing a viscous core (Tomar et al., 2011).

Acknowledgments

Supports from the National Natural Science Foundation of China (Grant Nos. 31270989 and 11172155), Tsinghua University (2012Z02103 and 20121087991) and 973 Program of MOST (2010CB631005) are gratefully acknowledged.

REFERENCES

Ben Amar, M., Goriely, A., 2005. Growth and instability in elastic tissues. Journal of the Mechanics and Physics of Solids 53 (10), 2284–2319.

Breid, D., Crosby, A.J., 2009. Surface wrinkling behavior of finite circular plates. Soft Matter 5 (2), 425–431.

Burger, E.J., Macklem, P., 1968. Airway closure-demonstration by breathing 100 percent O_2 at low lung volumes and by N_2 washout. Journal of Applied Physiology 25 (2), 139–148.

Dervaux, J., Ben Amar, M., 2011. Buckling condensation in constrained growth. Journal of the Mechanics and Physics of Solids 59 (3), 538–560.

Dervaux, J., Couder, Y., Guedeau-Boudeville, M.-A., Ben Amar, M., 2011. Shape transition in artificial tumors: from smooth buckles to singular creases. Physical Review Letters 107 (1), 018103.

Fayed, M.H., Elnasharty, M., Shoaib, M., 2010. Localization of sugar residues in the stomach of three species of monkeys (tupaiidae glis, nycticebus cocang and callithrix jacchus) by lectin histochemistry. International Journal of Morphology 28 (1), 111–120.

Heil, M., White, J.P., 2002. Airway closure: surface-tension-driven non-axisymmetric instabilities of liquid-lined elastic rings. Journal of Fluid Mechanics 462, 79–109.

Heil, M., Hazel, A.L., Smith, J.A., 2008. The mechanics of airway closure. Respiratory Physiology and Neurobiology 163 (1–3), 214–221.

Hill, M.J., Wilson, T.A., Lambert, R.K., 1997. Effects of surface tension and intraluminal fluid on mechanics of small airways. Journal of Applied Physiology 82 (1), 233–239.

Hrousis, C.A., Wiggs, B.J., Drazen, J.M., Parks, D.M., Kamm, R.D., 2002. Mucosal folding in biologic vessels. Journal of Biomechanical Engineering 124 (4), 334–341.

Jones, G.W., Chapman, S.J., 2012. Modeling growth in biological materials. SIAM Review 54 (1), 52–118.

Kang, M.K., Huang, R., 2010. Effect of surface tension on swell-induced surface instability of substrate-confined hydrogel layers. Soft Matter 6 (22), 5736–5742.

Lambert, R.K., Codd, S.L., Alley, M.R., Pack, R.J., 1994. Physical determinants of brochial mucosal folding. Journal of Applied Physiology 77 (3), 1206–1216.

Li, B., Cao, Y.P., Feng, X.Q., 2011a. Growth and surface folding of esophageal mucosa: a biomechanical model. Journal of Biomechanics 44 (1), 182–188.

Li, B., Cao, Y.P., Feng, X.Q., Gao, H.J., 2011b. Surface wrinkling of mucosa induced by volumetric growth: theory, simulation and experiment. Journal of the Mechanics and Physics of Solids 59 (4), 758–774.

Li, B., Cao, Y.P., Feng, X.Q., Gao, H.J., 2012. Mechanics of morphological instabilities and surface wrinkling in soft materials: a review. Soft Matter 8 (21), 5728–5745.

Li, B., Li, Y., Xu, G.K., Feng, X.Q., 2009. Surface patterning of soft polymer film-coated cylinders via an electric field. Journal of Physics: Condensed Matter 21 (44), 445006.

Liang, H.Y., Mahadevan, L., 2009. The shape of a long leaf. Proceedings of the National Academy of Sciences of the United States of America 106 (52), 22049–22054.

Liu, H.W., Hong, W, Suo, Z.G., Swaddiwudhipong, S., Zhang, Y.W., 2010. Modeling and simulation of buckling of polymeric membrane thin film gel. Computational Materials Science 49 (1), 60–64.

MacLaurin, J., Chapman, J., Jones, G.W., Roose, T., 2012. The buckling of capillaries in solid tumours. Proceedings of the Royal Society A 468 (2148), 4123–4145.

Moulton, D.E., Goriely, A., 2011. Circumferential buckling instability of a growing cylindrical tube. Journal of the Mechanics and Physics of Solids 59 (3), 525–537.

Ogden, R.W., 1984. Non-Linear Elastic Deformations. New York, Chichester.

Pham, K., Frieboes, H.B., Cristini, V., Lowengrub, J., 2011. Predictions of tumour morphological stability and evaluation against experimental observations. Journal of the Royal Society Interface 8 (54), 16–29.

Rodriguez, E.K., Hoger, A., McCulloch, A.D., 1994. Stress-dependent finite growth in soft elastic tissues. Journal of Biomechanics 27 (4), 455–467.

Savin, T., Kurpios, N.A., Shyer, A.E., Florescu, P., Liang, H.Y., Mahadevan, L., Tabin, C., 2011. On the growth and form of the gut. Nature 476 (7358), 57–63.

Sultan, E., Boudaoud, A., 2008. The buckling of a swollen thin gel layer bound to a compliant substrate. Journal of Applied Mechanics 75 (5), 051002.

Sutherland, R.M., 1988. Cell and environment interactions in tumor microregins—the multicell spheroid model. Science 240 (4849), 177–184.

Taber, L.A., 1995. Biomechanics of Growth, remodeling, and morphogenesis. Applied Mechanics Reviews 48 (8), 487–545.

Tanaka, T., Sun, S.-T., Hirokawa, Y., Katayama, S., Kucera., J., Hirose, Y., Amiya, T., 1987. Mechanical instability of gels at the phase transition. Nature 325 (6107), 796–798.

Tomar, G., Bandopadhayay, D., Sharma, A., 2011. Instabilities of soft elastic microtubes filled with viscous fluids: pearls, wrinkles, and sausage strings. Physical Review E 84 (3), 031603.

Tracqui, P., 2009. Biophysical models of tumour growth. Reports on Progress in Physics 72 (5), 056701.

Wiggs, B.R., Hrousis, C.A., Drazen, J.M., Kamm, R.D., 1997. On the mechanism of mucosal folding in normal and asthmatic airways. Journal of Applied Physiology 83 (6), 1814–1821.

Yang, W., Fung, T.C., Chian, K.S., Chong, C.K., 2007. Instability of the two-layered thick-walled esophageal model under the external pressure and circular outer boundary condition. Journal of Biomechanics 40 (3), 481–490.